

Titre: A wearable electrochemical aptasensor based MOF on MOF heterostructure for multi-neurotransmitters monitoring. Supplément
Title:

Auteurs: Zina Fredj, Fahimeh Marvi, Fateh Ullah, & Mohamad Sawan
Authors:

Date: 2025

Type: Article de revue / Article

Référence: Fredj, Z., Marvi, F., Ullah, F., & Sawan, M. (2025). A wearable electrochemical aptasensor based MOF on MOF heterostructure for multi-neurotransmitters monitoring. Microchimica Acta, 192, 384 (13 pages).
Citation: <https://doi.org/10.1007/s00604-025-07219-5>

Document en libre accès dans PolyPublie

Open Access document in PolyPublie

URL de PolyPublie: <https://publications.polymtl.ca/66072/>
PolyPublie URL:

Version: Matériel supplémentaire / Supplementary material
Révisé par les pairs / Refereed

Conditions d'utilisation: Creative Commons Attribution-Utilisation non commerciale-Pas d'oeuvre dérivée 4.0 International / Creative Commons Attribution-NonCommercial-NoDerivatives 4.0 International (CC BY-NC-ND)
Terms of Use:

Document publié chez l'éditeur officiel

Document issued by the official publisher

Titre de la revue: Microchimica Acta (vol. 192)
Journal Title:

Maison d'édition: Springer Science+Business Media
Publisher:

URL officiel: <https://doi.org/10.1007/s00604-025-07219-5>
Official URL:

Mention légale:
Legal notice:

A Wearable Electrochemical Aptasensor based MOF on MOF Heterostructures for Multi-neurotransmitters Monitoring

Zina Fredj¹, Fahimeh Marvi¹, Fateh Ullah¹, Mohamad Sawan^{1*}

¹ CenBRAIN Neurotech, School of Engineering, Westlake University, Hangzhou, 310030, China.

*Correspondence: sawan@westlake.edu.cn (M.S.)

Supplementary Information (SI)

Chemicals

Indium chloride tetrahydrate ($\text{InCl}_3 \cdot 4\text{H}_2\text{O}$), copper nitrate ($\text{Cu}(\text{NO}_3)_2$), 2-aminoterephthalic acid ($\text{H}_2\text{BDC-NH}_2$), polyvinylpyrrolidone K30 (PVP-K30), N,N-dimethylformamide (DMF), and ethanol were sourced from Sinopharm Chemical Reagent Co., Ltd. (Beijing, China). Tetrachloroauric acid trihydrate (HAuCl_4), 1,3,5-benzenetricarboxylic acid (H_3BTC), and sodium citrate were obtained from Macklin Biochemical Co., Ltd. (Shanghai, China). Additionally, MCH (6-mercapto-1-hexanol) was acquired from Aladdin Chemical (Beijing, China). Chemicals such as dopamine, serotonin (5-hydroxytryptamine), epinephrine, norepinephrine, uric acid, L-ascorbic acid, acetylcholine, glucose, and potassium chloride were purchased from Sigma-Aldrich (Beijing, China). Artificial sweat (pH 6.5) and PBS buffer (pH 7.2) were obtained from Fuzhou Feijing Biotechnology Co., LTD (China). All aptamers (sequences provided in **Table S1**) were procured from Sangon Biotech, Shanghai, China.

Table S1. Sequences of the involved oligonucleotide and probe

Name	Sequence (5'-3')
DA Apt	SH-C6- CGACGCCAGTTTGAAGGTTTCGTCGCAGGTGTGGAGTGACGTCG
5-HT Apt	SH-C6- CGACTGGTAGGCAGATAGGGGAAGCTGATTCGATGCGTGGGTTCG
Ep Apt	SH-C6- TACGTGAATCCATGGGGACGGAGAGACGGCACGAACCAA

Instruments

The structural and morphological properties of the synthesized material were analyzed using X-ray diffraction (Bruker D8 Discover), field emission-scanning electron microscopy (Zeiss Gemini 450), and Transmission Electron Microscopy with Energy-Dispersive X-ray Spectroscopy (Thermo Fisher Talos F200XG2). Surface elemental analysis was conducted using X-ray Photoelectron Spectroscopy (Thermo Fisher ESCALAB Xi⁺). The electrochemical analysis was

carried out using a Potentiostat (BioLogic VMP3 instruments with 16 channels) for electrochemical impedance spectroscopy (EIS) and voltammetric analyses. All experiments were conducted in a controlled dark environment at room temperature to maintain consistent conditions. Our investigation employed a new generation of flexible screen-printed carbon electrodes (SPCEs) featuring three working electrodes. The fabrication of these electrodes involves a layered structure, beginning with a first layer of polyimide (PI) material with a controlled thickness of 0.125 mm. This layer serves as the flexible and durable substrate for subsequent electrode deposition. The working electrodes and counter electrode are constructed using carbon ink, whereas the reference electrode is fabricated with silver ink. These ink choices contribute to the optimized performance of the three-electrode system. Each working electrode has a geometric area of 3.14 mm², emphasizing a balanced design for effective electrochemical responses.

The counter electrode and reference electrode feature geometric areas of 30.96 mm² and 2.16 mm², respectively, enhancing the overall versatility and efficiency of the flexible electrode system. The fabrication steps of the flexible electrode patch are detailed in the supplementary data. As illustrated in **Figure S1a**, the sequential steps involved in fabricating the flexible electrode patch are shown, while **Figure S1 b** provides the dimensions of the final product.

Fabrication Process of the SPE Array

The fabrication of a flexible electrode patch involves several precise steps to ensure optimal performance and structural integrity. This patch consists of three working electrodes, a reference electrode, and a counter electrode, integrated onto a flexible substrate (**Figure S1a**). A polyimide (PI) substrate is chosen for its excellent thermal stability, flexibility, and chemical resistance. The thickness of the PI substrate is 0.125 mm, providing a robust yet flexible base for the electrodes. Next, silver ink was deposited onto the PI substrate to form the conductive tracks that connect the various electrodes. Silver ink is preferred due to its high conductivity and good adhesion properties. The silver ink is applied using a screen-printing technique, ensuring precise and uniform patterns. The substrate with the printed silver ink is then cured at a specific temperature to solidify the conductive paths. Following the silver ink deposition, carbon ink is applied to form the working electrodes and the counter electrode.

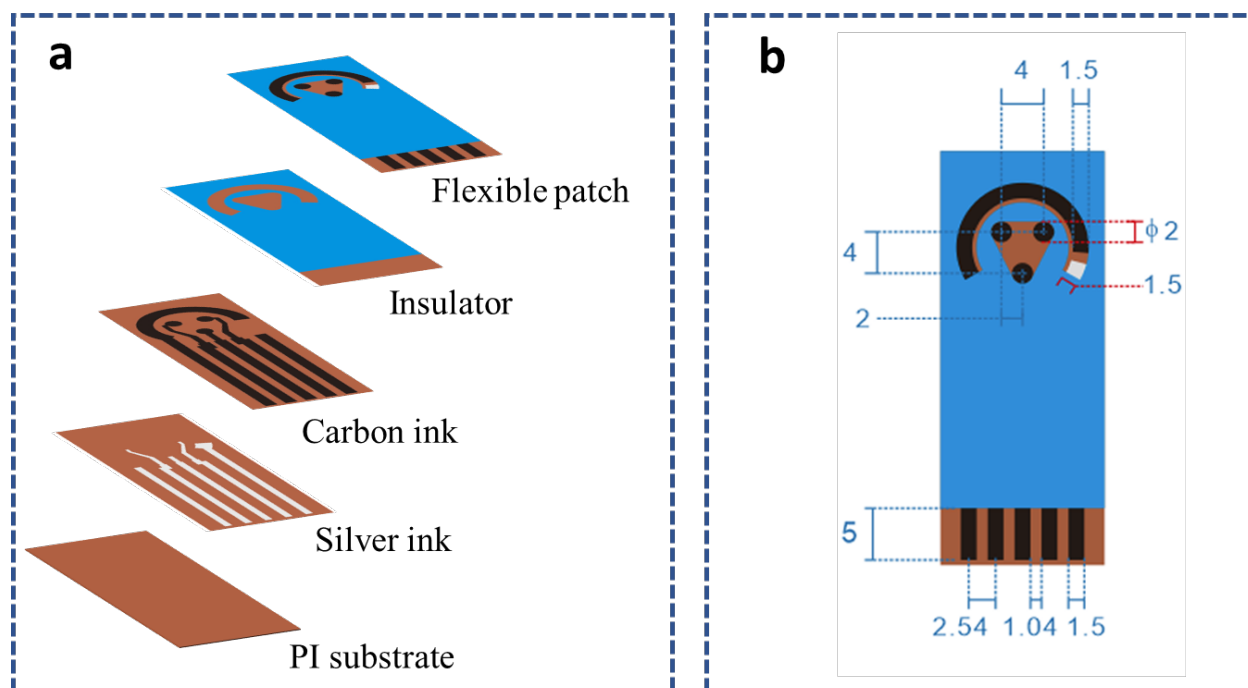


Figure S1. Flexible electrode Patch: a) Fabrication steps, b) Dimensions of the final product.

Carbon ink is chosen for its excellent electrochemical properties, stability, and cost-effectiveness. The carbon ink is also applied using a screen-printing technique, which allows for precise control over the electrode geometry. The working electrodes are designed with a geometric area of 3.14 mm² each, while the counter electrode has a larger geometric area of 30.96 mm². After printing, the carbon ink is cured to ensure strong adhesion to the substrate. The reference electrode is fabricated using silver ink with a geometric area of 2.16 mm². Similar to the previous steps, the silver ink is deposited using screen-printing and then cured to achieve the desired electrical properties. An insulation layer is then applied over the entire structure, leaving only the active areas of the electrodes exposed (**Figure S1b**). This insulating layer protects the conductive tracks and prevents any unintended electrical interactions. The insulation material is carefully chosen to provide adequate protection while maintaining the flexibility of the patch. It is applied uniformly and cured to form a stable protective layer. After the application and curing of the insulation layer, the final product undergoes rigorous inspection to ensure all specifications are met.

AuNPs electrodeposition

The gold electrodeposition process onto the CuMOF@InMOF-modified electrode was carried out using cyclic voltammetry (CV) to ensure a uniform and controlled deposition of gold nanoparticles (AuNPs). The CV technique was applied in a standard electrolyte solution containing a gold precursor, using a potential range of 0 to 0.8. This method was chosen due to its ability to control both the amount and distribution of AuNPs on the CuMOF@InMOF surface, enhancing the sensor's conductivity and sensitivity. As shown in the CV graph (Figure S2), the redox peaks indicate the successful deposition of gold on the electrode surface. The prominent peak observed around 350 mV corresponds to the reduction of the gold ions to form AuNPs, while the broad oxidation peak signifies the stabilization of the gold film on the electrode surface. The number of cycles and the applied potential were carefully selected to ensure the optimal size and distribution of the AuNPs, maximizing the sensor's electrochemical performance for neurotransmitter detection. This CV-based deposition process improves upon traditional chemical deposition methods by offering precise control over the thickness and morphology of the gold layer. The deposited AuNPs enhance the electrochemical activity of the CuMOF@InMOF platform, leading to improved electron transfer rates and signal amplification in subsequent detection processes.

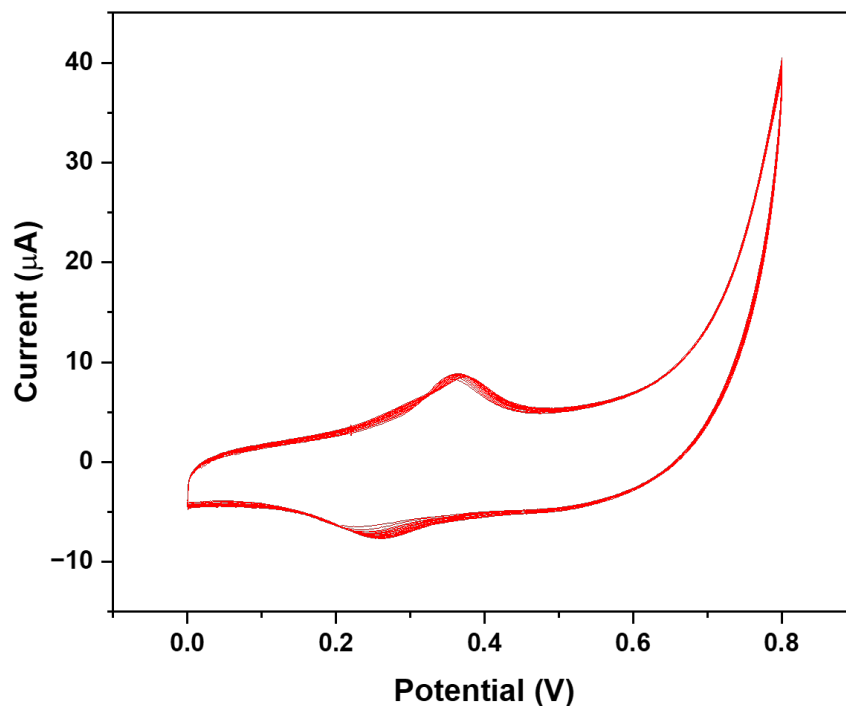


Figure S2. Cyclic voltammetry profile for gold electrodeposition onto CuMOF@InMOF.

Morphological Characterization of Individual MOFs

Figure S3 presents SEM images of the individual metal-organic frameworks used in the construction of the CuMOF@InMOF heterostructure. Figure S3a shows the InMOF, which exhibits a well-defined rod-like morphology with uniform dimensions. Figure S3b displays CuMOF particles characterized by a spherical shape and nanoscale diameter. These distinct morphologies confirm the successful synthesis of the separate MOF components prior to integration into the composite structure.

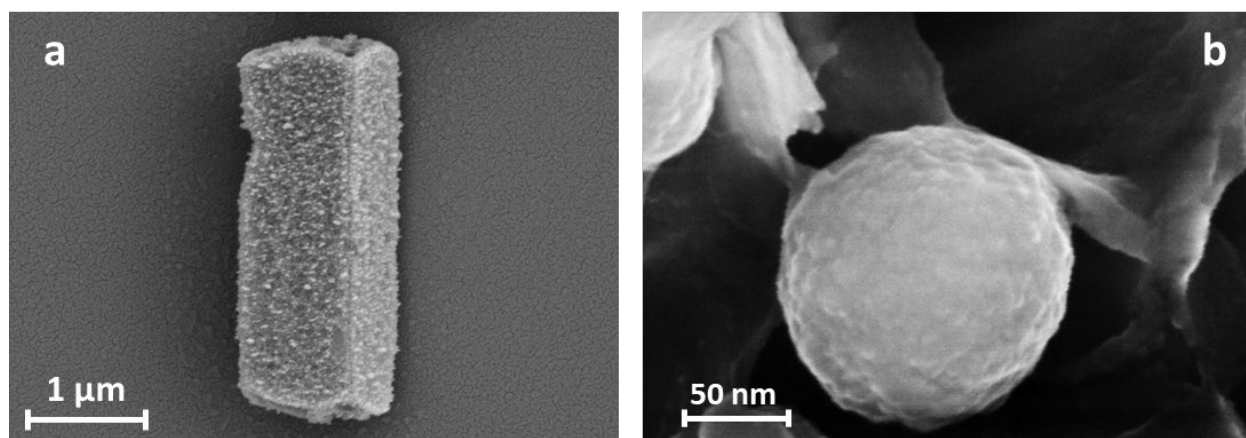


Figure S3. SEM images of individual MOF components used in the synthesis of the CuMOF@InMOF heterostructure: a) SEM image of InMOF showing a rod-like morphology, b) SEM image of CuMOF displaying a spherical morphology.

Microfluidic integration

We developed a microfluidic model, designed using AutoCAD, specifically optimized for the continuous collection of sweat samples and the efficient delivery of neurotransmitters to the detection zone for analysis (**Figure S4**). The microfluidic structure features a central circular chamber with a radius of 6.0 mm, connected to 12 inlets that enable the collection of sweat from various areas. The inlet channels are designed with varying radii to ensure even distribution and fluid flow, with the smaller inlet radii set at 0.8 mm for optimal capillary action and fluid transport. Each inlet is connected to an outer collection node, allowing for individual entry points of sweat, which is funneled into the central chamber through channels with a width of 0.5 mm.

The outlet, which facilitates sweat evacuation, has a channel width of 0.6 mm to ensure steady flow without clogging. This design improves upon previously published microfluidic systems in wearable biosensors by introducing more inlets, enhancing sweat collection, and enabling continuous monitoring. Compared to other models that typically utilize fewer inlets or rely on passive diffusion, this structure's multiple channels provide superior fluid management, particularly under low-sweat conditions. Furthermore, the precise control of channel dimensions and radii allows for more consistent flow rates, which is critical for real-time monitoring in physiological applications. In comparison with previous designs, this microfluidic model ensures a stable and reliable sample collection, improving the accuracy of on-body sweat analysis for neurotransmitter detection.



Figure S4. Custom-designed microfluidic layout for sweat collection and neurotransmitter monitoring (dimensions in mm). The design features a central circular chamber (radius: 6.0 mm) connected to twelve inlet channels and a single outlet channel, enabling efficient fluid distribution and collection.

This structure allows for efficient sweat collection and delivery to the biosensor, ensuring continuous monitoring under physiological conditions. As illustrated in **Figure S5**, the microfluidic module is composed of three distinct layers: an adhesive layer, a spacer, and a layer

containing the microfluidic channels. These layers are assembled to form the complete microfluidic system designed for efficient sweat collection and neurotransmitter analysis. The microfluidic module was fabricated using PET (Polyethylene Terephthalate) film, which was patterned using a CO₂ laser cutter to ensure high precision. The adhesive layer, responsible for bonding the microfluidic module to the skin or the device surface, was constructed from PET film with double-sided tape (dimensions: 2.00 cm × 2.00 cm × 0.14 mm). This adhesive ensures a tight seal, preventing leakage while maintaining flexibility for wearable applications. The spacer, fabricated from PET film (dimensions: 2.00 cm × 2.00 cm × 0.015 mm), provides the necessary gap between the adhesive layer and the microfluidic channels, ensuring proper flow of sweat through the device. Finally, the patterned PET layer containing the microfluidic channels (dimensions: 2.00 cm × 2.50 cm × 0.15 mm) was also laser-cut using a CO₂ cutter. This layer features precisely etched channels that guide the collected sweat from the multiple inlets towards the detection zone. Following fabrication, the assembled microfluidic module is aligned and bonded to the aptamer-functionalized biosensor surface. An outlet PET layer (2.00 cm × 2.50 cm × 0.15 mm) is then added to complete the module, enabling directional flow and avoiding backpressure. The final structure supports on-body monitoring under physiological conditions with precise analyte delivery to the detection region.

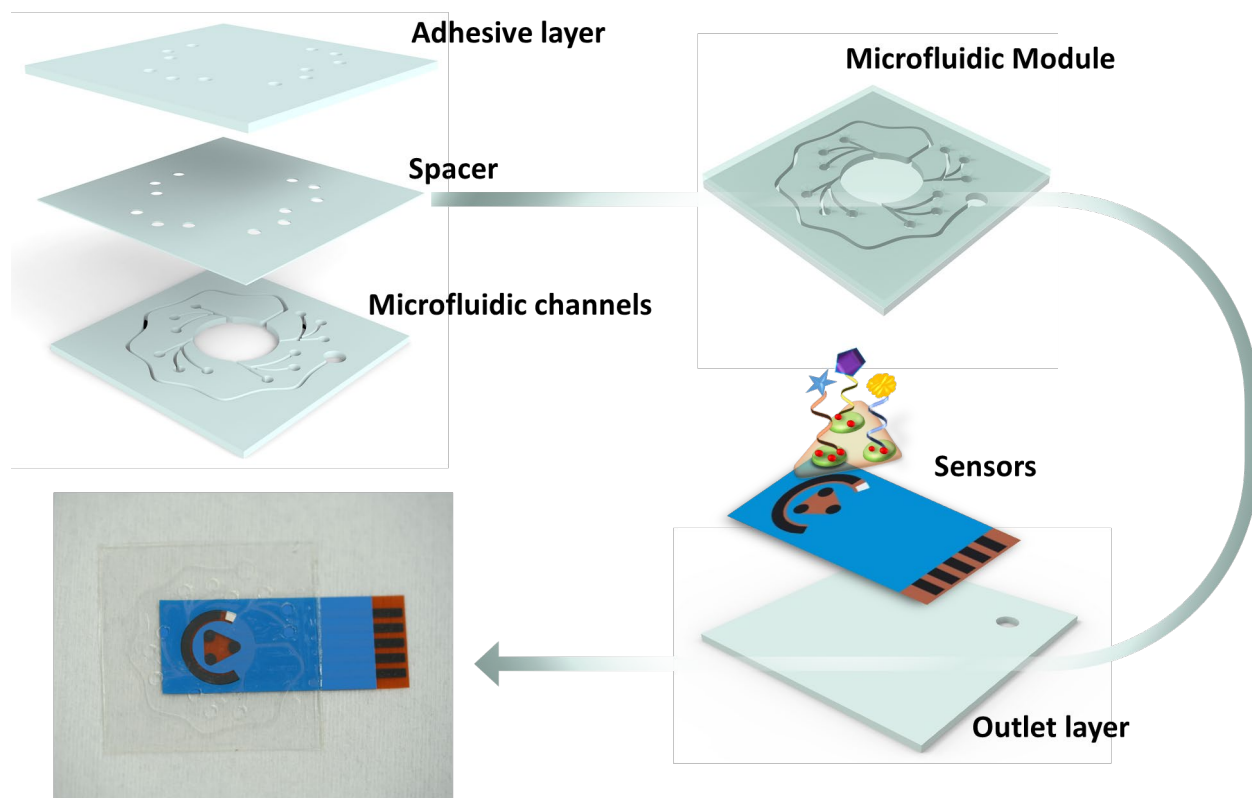


Figure S5. Microfluidic integration with the biosensor. The multilayer PET-based microfluidic module is laser-cut, assembled, and aligned with the electrode to enable real-time sweat sampling and neurotransmitter detection

On-Body neurotransmitters monitorin

To evaluate the practical application of the developed biosensor in real-time, on-body monitoring, a wearable sensing protocol was implemented. The flexible patch was adhered to the subject's forearm during physical activity to enable sweat collection and in situ neurotransmitter detection. The acquired signals were processed using a multi-channel electrochemical workstation. The full setup and workflow are illustrated in **Figure S6**.

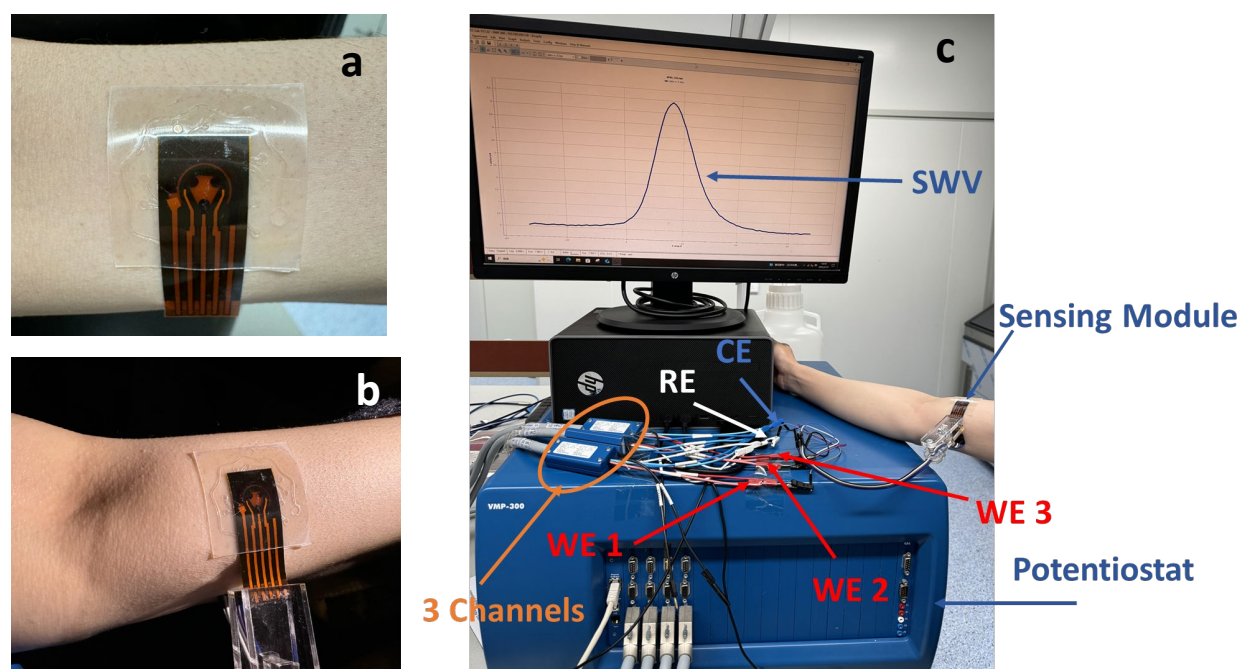


Figure S6. Wearable neurotransmitter monitoring setup: a) The flexible sensor patch adhered to the forearm prior to exercise, b) Connection of the patch to the electrochemical workstation immediately following exercise, enabling sweat collection, c) multi-channel electrochemical data acquisition using a VMP-300 potentiostat, with three working electrodes (WE1–WE3), one reference electrode (RE), and one counter electrode (CE). Real-time SWV signals are displayed on the computer interface.

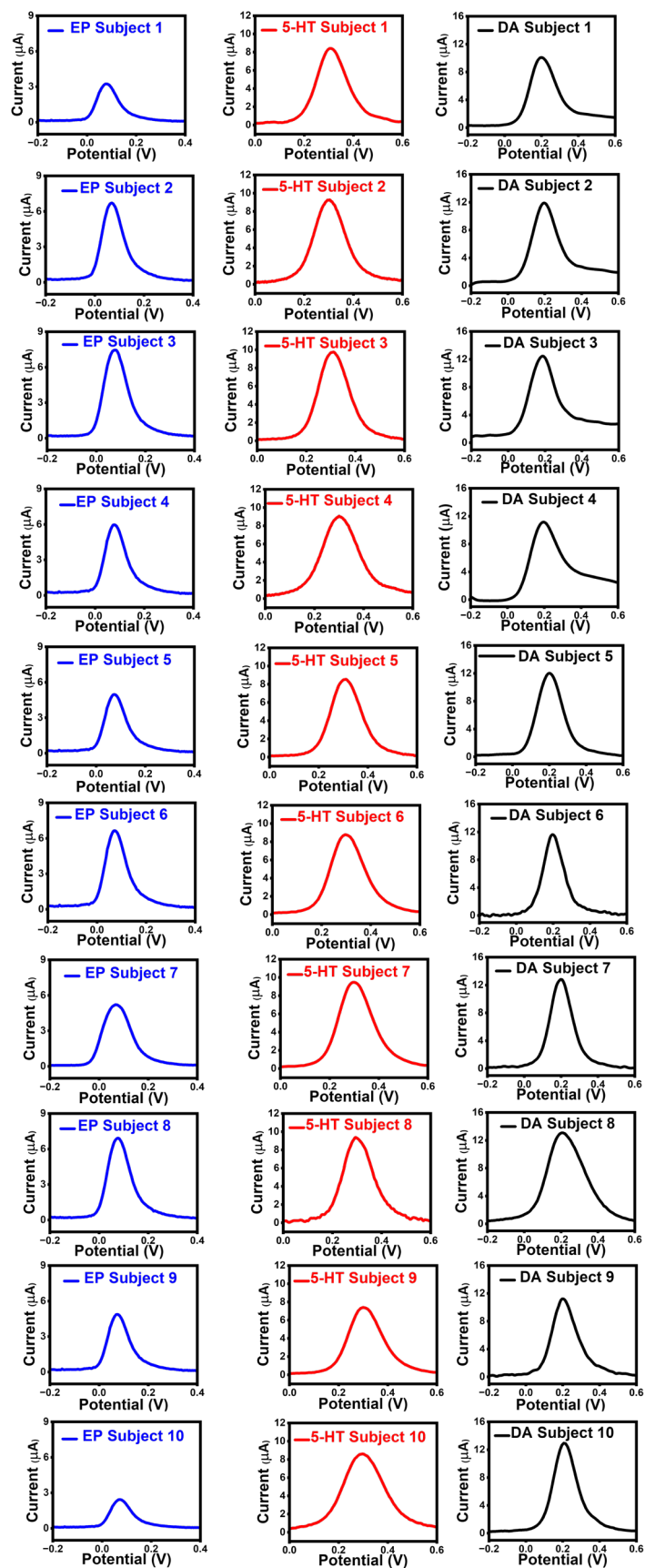


Figure S7. On-body SWV responses for epinephrine (EP), serotonin (5-HT), and Dopamine (DA) collected from 10 individual human subjects using the wearable biosensor patch. Each plot represents the electrochemical signal detected directly from sweat after physical activity, demonstrating consistent and distinguishable oxidation peaks for the three neurotransmitters across multiple subjects.

Table S2. Comparison of analytical performance of electrochemical sensors for neurotransmitters

NTs	Electrode materials	Technique	Sample Matrix	LOD	Ref
DA,5-HT	Aptamers-In ₂ O ₃ nanoribbon field-effect transistors	Amperometry	Sweat	10 fM 10 fM	[8]
DA,5HT	Aptamers-Graphene field-effect transistors	Amperometry	PBS	10 pM 10 pM	[9]
DA,5-HT	Aptamer-Au microelectrodes	SWV	PBS	0.1 µM 0.5 µM	[10]
EP	PEDOT–	CV	Urine	5.7 µM	[28]
5-HT	AuNPs/GCE			1.4 µM	
5-HT, EP	Poly Victoria blue B/ CPE	DPV	PBS	0.89 µM 0.33 µM	[29]
DA	SWCNT/GCE	CV	PBS	3.02 nM	[30]
5-HT				0.54 nM	
DA,5-HT	Aptamers-Au electrodes	DPV	Serum	0.06 µM 0.12 µM	[31]
DA,5-HT, EP	SPCE-CuMOF@InMOF-AuNPs-Apt	SWV Amperometry	Sweat	0.18 nM 0.33 nM 0.27 nM	This work

Glassy Carbon Electrode (GCE); Carbon Paste Electrode (CPE); Single-Walled Carbon Nanotube (SWCNT), Differential Pulse Voltammetry (DPV); Phosphate-Buffered Saline (PBS).